ISSN 1070-3284, Russian Journal of Coordination Chemistry, 2022, Vol. 48, No. 1, pp. 41–51. © Pleiades Publishing, Ltd., 2022.
Russian Text © The Author(s), 2022, published in Koordinatsionnaya Khimiya, 2022, Vol. 48, No. 1, pp. 45–56.

Synthesis and Structures of Disulfanilamide Glyoxime and Ni(II) and Cu(II) Complexes with This Ligand Stimulating the Proteolytic Properties of $[Cu(DsamH_2)_3]SO_4 \cdot 5H_2O$

P. N. Bourosh[a, b, *], Ed. B. Coropceanu[c], A. P. Rija[b], D. Ureche[b], A. A. Ciloci[d], S. F. Clapco[d], E. G. Dvornina[d], S. V. Labliuc[d], and I. I. Bulhac[b]

[a] *Institute of Applied Physics, Chisinau, Republic of Moldova*
[b] *Institute of Chemistry, Chisinau, Republic of Moldova*
[c] *Tiraspol State University, Chisinau, Republic of Moldova*
[d] *Institute of Microbiology and Biotechnology, Chisinau, Republic of Moldova*
**e-mail: pavlina.bourosh@ifa.md*

Received May 12, 2021; revised June 23, 2021; accepted June 28, 2021

Abstract—The reaction of dichloroglyoxime with sulfanilamide affords new glyoxime: disulfanilamide glyoxime ($DsamH_2$, L). Two coordination compounds are synthesized from $DsamH_2$: $[Ni(DsamH)_2]\cdot 2H_2O$ (**I**) and $[Cu(DsamH_2)_3]SO_4\cdot 5H_2O$ (**II**). Their compositions and structures are determined by elemental analysis and IR, UV, and NMR spectroscopy. Compounds L and **II** are studied by XRD (CIF files CCDC nos. 2080777 and 2080778, respectively). Both bis(ligand) and tris(ligand) complexes with L are synthesized depending on the synthesis conditions. The different degrees of deprotonation of the $DsamH_2$ ligand in complexes **I** and **II** cause the formation of both molecular and ionic complexes. Complex **II** taken in optimum concentrations exerts a stimulating effect on the protease synthesis of the biotechnologically significant micromycete strains *Fusarium gibbosum* CNMN FD 12 and *Trichoderma koningii* Oudemans CNMN FD 15.

Keywords: disulfanylamide glyoxime, coordination compounds of nickel(II) and copper(II), structural studies, microscopic fungi, proteases

DOI: 10.1134/S1070328422010018

INTRODUCTION

Coordination compounds of *d* metals with chelating ligands attract attention due to their stability provided by the stability of the carcass formed around the central metal ion in both the solid state and solutions [1–3]. The contributions of both the metal atom and polydentate and mixed ligands to the formation of the complexes can be distinguished [2, 4]. A series of the recent studies confirms that a large variety of the compounds with dioximes was mainly synthesized by the introduction of additional ligands affording mono- [2, 5], di- [6–8], and polynuclear homometallic complexes [9, 10]. Interest in the compounds with dioximes is also supported by possibilities of using them as models of physiologically important substances [11, 12] and in microbiology [13, 14], medicine [15], and agriculture [16]. The luminescence properties of the compounds of this class have recently been studied as well [9, 10]. The diversification of dioximes, especially an increase in their volume due to the addition of donor groups, affects both the compositions and structures of the coordination compounds and their properties, including biological properties [17–19].

A promising trend in the reproduction of natural biosynthesis is associated with the synthesis of chemical compounds that could be used as models of biological objects by studying their effect on metabolic processes of microorganisms. The insertion of diverse Co(III) dioximates into nutrient media of some microorganisms was found to stimulate enzyme biosynthesis in strain-producers and to increase biomass accumulation [14, 20]. Thus, an urgent task is the study of the biological activity of new coordination compounds with metals in order to reveal their possible practical use. The results obtained by the study can serve as a theoretical basis for the purposeful synthesis of the compounds with specified properties.

New dioxime, disulfanilamide glyoxime ($DsamH_2$, L), was synthesized by the condensation of dichloroglyoxime with sulfanilamide. The reactions of $DsamH_2$ with nickel chloride and copper(II) sulfate afforded coordination compounds $[Ni(DsamH)_2]\cdot 2H_2O$ (**I**) and $[Cu(DsamH_2)_3]SO_4\cdot 5H_2O$ (**II**), respectively. Their compositions and structures were determined by elemental analysis and IR, UV, and NMR spectroscopy. The crystal structures of compounds L

and **II** were determined by XRD. Compound **II** was tested as an agent stimulating the protease synthesis of the biotechnologically significant micromycete strains *Fusarium gibbosum* CNMN FD 12 and *Trichoderma koningii* Oudemans CNMN FD 15.

EXPERIMENTAL

Reagents ($NiCl_2 \cdot 2H_2O$, $CuSO_4 \cdot 5H_2O$, NaOH, Na_2CO_3, and sulfanilamide), a 25% ammonia solution, and solvents (reagent grade) purchased from commercial sources and synthesized dichloroglyoxime were used as received.

Synthesis of $DsamH_2$ (L) was carried out using a described procedure [21, 22] but with a longer stirring for 5–6 h. The yield was 0.28 g (63%). The substance is soluble in DMF and DMSO and less soluble in alcohols.

For $C_{14}H_{16}N_6O_6S_2$

Anal. calcd., %	C, 39.25	H, 3.76	N, 19.62
Found, %	C, 39.14	H, 3.58	N, 19.54

Compounds **I** and **II** were synthesized using a described procedure [22].

Synthesis of $[Ni(DsamH)_2] \cdot 2H_2O$ (I). A solution of $NiCl_2 \cdot 6H_2O$ (0.06 g, 0.25 mmol) in methanol (15 mL) was added to a warm solution of disulfanilamide glyoxime (0.214 g, 0.5 mmol) in methanol (30 mL). The mixture was stirred at 60°C for 15 min. Ammonia (5–6 droplets) was added with stirring after which a brown precipitate formed in the solution. The precipitate was filtered off, washed with cold methanol and ether, and dried in air. The yield was 0.2 g (43%). The substance is soluble in DMF and DMSO but is poorly soluble in methanol. Qualitative single crystals suitable for XRD were not obtained probably because of a weak solubility of the complex in easily volatile solvents.

For $C_{28}H_{34}N_{12}O_{14}S_4Ni$

Anal. calcd., %	C, 35.41	H, 3.61	N, 17.70	Ni, 6.18
Found, %	C, 35.47	H, 3.54	N, 17.62	Ni, 5.92

Synthesis of $[Cu(DsamH_2)_3]SO_4 \cdot 5H_2O$ (II). Disulfanilamide glyoxime (0.214 g, 0.5 mmol) was dissolved in methanol (40 mL), and the solution was heated to 60°C in a water bath (solution 1). Copper(II) sulfate pentahydrate (0.063 g, 0.25 mmol) was dissolved in a minimum amount of water, and methanol (20 mL) was added (solution 2). Solution 2 was added dropwise to solution 1 with permanent stirring, and the resulting solution was filtered and left to stay for slow evaporation at room temperature. Crystals as elongated plates were formed in the solution within 5 days. The yield was 0.4 g (52%). The substance is weakly soluble in DMF and DMSO.

For $C_{42}H_{58}N_{18}O_{27}S_7Cu$

Anal. calcd., %	C, 32.86	H, 3.81	N, 16.42	Cu, 4.14
Found, %	C, 32.72	H, 3.71	N, 16.34	Cu, 3.99

The compositions and structures of compounds L, **I**, and **II** were determined by elemental analysis and UV and NMR spectroscopy, and those for the single crystals of compounds L and **II** were determined by XRD. IR spectra were recorded on an FT-IR Perkin-Elmer Spectrum 100 instrument in Nujol in a range of 4000–400 cm^{-1} and in a range of 4000–650 cm^{-1} for the ATR-mode. UV spectra were detected on a Perkin-Elmer Lambda 25 spectrophotometer. ^1H and ^{13}C NMR spectra were recorded on a 400 Bruker spectrometer with the working frequency 400.13 MHz for ^1H and 100.61 MHz for ^{13}C in DMSO-d_6 solutions using TMS as the internal standard. The signals were given in ppm.

XRD. Experimental data for compounds L and **II** were obtained at room temperature (293(2) K) on an Xcalibur E diffractometer (MoK_α radiation, graphite monochromator). The unit cell parameters were refined over the whole set, and other experimental data were obtained using the CrysAlis Oxford Diffraction software [23]. The structures of the compounds were solved by direct methods and refined by least squares in the anisotropic full-matrix approximation for nonhydrogen atoms (SHELX-97) [24]. The positions of the hydrogen atoms of the solvate water molecules were determined from the difference Fourier synthesis, and those of other hydrogen atoms were calculated geometrically. All hydrogen atoms were isotropically refined in the rigid body model with $U_{eff} = 1.2U_{equiv}$ or $1.5U_{equiv}$ of the corresponding atoms (C, N, and O). The experimental and structure refinement characteristics for compounds L and **II** are given in Table 1. Selected interatomic distances and bond angles are listed in Table 2. The geometric parameters of intermolecular hydrogen bonds are given in Table 3.

The positional and thermal parameters of atoms in compounds L and **II** were deposited with the Cambridge Crystallographic Data Centre (CIF files CCDC nos. 2080777 and 2080778, respectively); deposit@ccdc.cam.ac.uk or http://www.ccdc.cam.ac.uk/data_request/cif).

Biological methods. The objects of the study were strains of the mycelium fungi *Fusarium gibbosum* CNMN FD 12 and *Trichoderma koningii* Oudemans CNMN FD 15, which are active producers of a complex of proteolytic enzymes (acidic, neutral, and alkaline proteases) [25, 26]. The strains are stored in the National Collection of Nonpathogenic Microorganisms of the Republic of Moldova at the Institute of Microbiology and Biotechnology.

Table 1. Crystallographic data and experimental characteristics for compounds L and **II**

Parameters	L	**II**
Empirical formula	$C_{14}H_{16}N_6O_6S_2$	$C_{42}H_{58}N_{18}O_{27}S_7Cu$
FW	428.45	1535.02
Crystal system	Trigonal	Monoclinic
Space group	$P3_12_1$	$P2_1/c$
a, Å	8.2460(3)	15.3303(9)
b, Å	8.2460(3)	14.9756(7)
c, Å	23.6703(17)	28.782(2)
α, deg	90	90
β, deg	90	97.818(6)
γ, deg	120	90
V, Å^3	1393.85(12)	6546.4(7)
Z	3	4
ρ_{calc}, g/cm^3	1.531	1.557
μ, mm^{-1}	1.027	0.651
F(000)	666	3172
Crystal size, mm	0.18 × 0.18 × 0.12	0.50 × 0.30 × 0.02
Range of θ, deg	2.98–25.50	2.86–25.05
Index ranges	$-9 \le h \le 5$, $-3 \le k \le 9$, $-17 \le l \le 28$	$-18 \le h \le 17$, $-10 \le k \le 17$, $-34 \le l \le 26$
Number of measured/independent reflections (R_{int})	2472/1680 (0.0263)	24527/11594 (0.0932)
Number of reflections with $I > 2\sigma(I)$	1524	3262
Completeness, %	99.8 (θ = 25.50°)	99.9 (θ = 25.05°)
Number of refined parameters	128	876
GOOF	1.000	1.007
R factors ($I > 2\sigma(I)$)	$R_1 = 0.0471$ $wR_2 = 0.1002$	$R_1 = 0.0632$ $wR_2 = 0.1429$
R factors (for all data)	$R_1 = 0.0542$ $wR_2 = 0.1073$	$R_1 = 0.2095$ $wR_2 = 0.1830$
$\Delta\rho_{max}/\Delta\rho_{min}$, e Å^{-3}	0.243/–0.302	0.870/–0.430

The producers were cultivated by the deep method.

The activity of the acidic (pH 3.6) and neutral (pH 7.4) proteases in the cultural liquid was determined by the Wilschtetter method based on the determination of the amount of free carboxyl groups formed by the hydrolysis of a 5% solution of gelatin. The amount of enzyme formed from 1 mg of amine nitrogen within 1 h under standard experimental con-

Table 2. Interatomic distances (*d*) and bond angles (ω) in compound **II** and ligand L

In coordination polyhedron of Cu(II) in compound **II**			
Bond	*d*, Å	Bond	*d*, Å
Cu(1)–N(1)	2.019(6)	Cu(1)–N(4)	1.989(6)
Cu(1)–N(2)	1.978(6)	Cu(1)–N(5)	2.005(6)
Cu(1)–N(3)	2.508(5)	Cu(1)–N(6)	2.282(6)
Angle	ω, deg	Angle	ω, deg
N(1)CuN(2)	79.6(3)	N(2)CuN(6)	100.6(2)
N(1)CuN(3)	100.0(2)	N(3)CuN(4)	71.4(3)
N(1)CuN(4)	168.8(2)	N(3)CuN(5)	82.4(3)
N(1)CuN(5)	94.9(3)	N(3)CuN(6)	154.2(2)
N(1)CuN(6)	91.0(2)	N(4)CuN(5)	91.0(2)
N(2)CuN(3)	104.3(2)	N(4)CuN(6)	99.9(2)
N(2)CuN(4)	95.4(3)	N(5)CuN(6)	73.3(2)
N(2)CuN(5)	171.9(3)		

In fragments of organic molecule L and coordinated ligand in compound **II**				
Bond	L	**II**		
	d, Å			
N(1)–C(1)	1.283(5)	1.299(9)	1.298(9)	1.302(9)
N(1)–O(1)	1.421(4)	1.379(7)	1.394(6)	1.388(7)
N(2)–C(2)		1.311(9)	1.311(9)	1.296(9)
N(2)–O(2)		1.395(7)	1.399(6)	1.418(8)
C(1)–C(1)*/C(2)	1.488(8)	1.480(10)	1.489(9)	1.495(10)
Angle	ω, deg			
O(1)N(1)C(1)	108.7(3)	112.9(6)	111.3(6)	113.0(6)
O(2)N(2)C(2)		110.9(6)	111.2(5)	110.1(7)
N(1)C(1)C(1)*/(2)	115.3(3)	113.7(7)	113.3(7)	111.2(7)
N(2)C(2)C(1)		109.6(6)	114.5(6)	112.0(7)

ditions were accepted to be the proteolytic activity unit [27]. The statistical processing of the results was performed by the Dospekhov method using computer programs [28].

RESULTS AND DISCUSSION

Disulfanilamide glyoxime was synthesized by the condensation of dichloroglyoxime with sulfanilamide in a molar ratio of 1 : 2 (Scheme 1) [22].

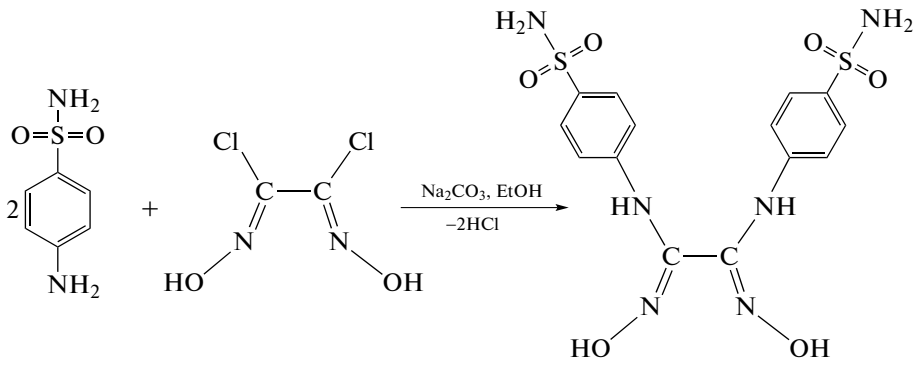

Scheme 1.

Table 3. Geometric parameters of intermolecular hydrogen bonds in the structures of compounds L and **II**

Contact D–H···A	Distance, Å			Angle DHA, deg	Symmetry transforms for A
	D–H	H···A	D···A		
L					
O(1)–H(1)···O(2)	0.82	2.03	2.838(5)	167	$-x + y + 1, -x, z - 1/3$
N(2)–H(1)···O(3)	0.86	2.35	3.122(5)	149	x, y, z
N(3)–H(2)···N(1)	0.96	2.11	3.028(5)	158	$-x + 2, -x + y + 2, -z + 1/3$
N(3)–H(1)···N(3)	0.92	2.11	3.004(5)	163	$x - y + 1, -y + 1, -z + 2/3$
II					
O(1)–H(1)···O(2*S*)	0.82	1.75	2.563(7)	171	x, y, z
O(2)–H(2)···O(4*S*)	0.82	1.79	2.605(7)	177	$-x + 2, y + 1/2, -z + 3/2$
O(3)–H(3)···O(3*S*)	0.82	1.94	2.762(7)	174	x, y, z
O(4)–H(4)···O(3*S*)	0.82	1.83	2.651(7)	178	$-x + 2, y + 1/2, -z + 3/2$
O(5)–H(5)···O(1*w*)	0.79	2.31	2.936(7)	137	x, y, z
O(6)–H(6)···O(3)	0.82	2.46	3.142(7)	141	$-x + 2, y + 1/2, -z + 3/2$
N(11)–H(1)···O(11)	0.86	2.33	3.049(12)	141	$-x + 2, -y + 1, -z + 1$
N(21)–H(2)···O(62)	0.86	2.47	3.224(12)	150	$x + 1, y, z$
N(22)–H(1)···O(32)	0.86	2.17	2.853(11)	136	$-x + 3, y - 1/2, -z + 3/2$
N(22)–H(2)···O(1*w*)	0.86	2.21	3.025(9)	158	$-x + 2, y - 1/2, -z + 3/2$
N(31)–H(1)···O(2*w*)	0.86	2.36	3.161(10)	156	$-x + 2, y - 1/2, -z + 3/2$
N(32)–H(1)···O(12)	0.90	2.53	3.276(13)	141	$x, -y + 3/2, z + 1/2$
N(41)–H(1)···O(3*w*)	0.86	2.27	3.054(10)	151	$-x + 2, y + 1/2, -z + 3/2$
N(42)–H(2)···O(1*S*)	0.90	1.95	2.739(11)	145	$-x + 2, -y + 1, -z + 2$
N(51)–H(1)···O(3*w*)	0.86	2.07	2.905(8)	162	x, y, z
N(52)–H(2)···O(7*w*)	0.86	1.98	2.82(2)	166	x, y, z
N(61)–H(2)···O(2*w*)	0.86	2.11	2.935(9)	161	x, y, z
O(1*w*)–H(1)···O(52)	0.85	2.04	2.815(9)	151	$-x + 1, y - 1/2, -z + 3/2$
O(1*w*)–H(2)···O(1*S*)	0.93	2.01	2.934(9)	171	x, y, z
O(2*w*)–H(1)···O(21)	0.83	2.01	2.845(10)	179	$-x + 2, -y + 1, -z + 1$
O(2*w*)–H(2)···O(42)	0.87	2.03	2.899(11)	179	$x, -y + 3/2, z - 1/2$
O(3*w*)–H(1)···O(4*w*)	0.87	2.06	2.929(14)	180	$-x + 2, -y + 1, -z + 1$
O(3*w*)–H(2)···O(2*S*)	0.90	2.08	2.979(9)	179	x, y, z
O(4*w*)–H(1)···O(6*w*)	0.85	1.85	2.70(2)	179	$-x + 3, -y + 1, -z + 1$
O(4*w*)–H(2)···N(32)	0.88	2.48	3.16(2)	134	$x, -y + 3/2, z - 1$
O(5*w*)–H(1)···O(4*S*)	0.92	1.86	2.77(2)	170	$x, y + 1, z$
O(5*w*)–H(2)···O(51)	0.85	1.86	2.71(2)	179	x, y, z
O(6*w*)–H(1)···O(6*w*)	0.85	2.31	3.16(4)	173	$-x + 3, -y + 1, -z + 1$
O(6*w*)–H(2)···N(12)	0.90	2.46	3.26(3)	148	x, y, z
O(6*w*)–H(2)···O(12)	0.90	2.43	3.26(2)	152	x, y, z
O(7*w*)–H(1)···O(61)	0.85	2.59	3.34(2)	177	x, y, z
O(7*w*)–H(2)···O(1*S*)	0.85	2.48	3.33(2)	179	$-x + 1, y + 1/2, -z + 3/2$

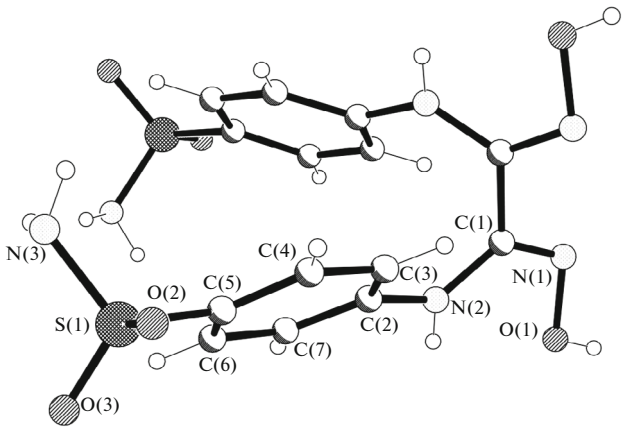

Fig. 1. Structure of the $DsamH_2$ molecule and notation of crystallographically independent atoms in L.

The IR spectrum of $DsamH_2$ contains bands at 3424, 3357, 3283 ν(NH), and 3076 cm^{-1} ν(OH) shifted toward lower frequencies due to molecular associations of the oxime NOH and NH groups and bands at 1642 ν(C=N), 1592 $\nu(CC)_{arom}$, 1302, 1150 ν(SO), 935 ν(NO), and 767, 725 cm^{-1} δ(CH) [29–32].

In the ^1H NMR spectrum of $DsamH_2$, two doublets at 7.54 ppm (2H, $J = 8.78$ Hz) and 6.89 ppm (2H, $J = 8.78$ Hz) belong to the aromatic ring, the signal at 7.16 ppm corresponds to the NH_2 group, and the signal at 8.77 ppm belongs to the NH group of the sulfanilamide fragment. The results of the examination of the ^1H NMR spectrum confirm that the condensation of sulfanilamide with dichlorodioxime proceeds via the NH_2 group directly bound to the aromatic ring, since this group undergoes the strongest downfield shift, and the loss of a proton of this group becomes noticeable upon signal integration. The signal corresponding to the oxime group protons is observed at 10.89 ppm. In the ^{13}C NMR spectrum of $DsamH_2$, the signals at 118.71 and 126.77 ppm correspond to the tertiary carbon atoms: those at 136.17 and 143.01 ppm correspond to the carbons of the aromatic ring, and the signal at 142.50 ppm belongs to the oxime carbon atom.

The reactions of the copper or nickel salts with disulfanilamide glyoxime gave two different complexes: nickel bis(dioximate) and copper tris(dioximine), since it was taken into account that tris(dioximines) were formed at pH ~2, whereas pH ~5–6 is characteristic of the formation of bis(dioximates). A weakly acidic medium was obtained by the addition of 1–2 droplets of an ammonia solution, and the addition of hydrochloric acid provided an acidic medium similarly to the formation of the complexes with dianilineglyoxime [33].

In the case of Ni(II) dioximate with $DsamH_2$, the UV spectrum exhibits bands at 202 and 280 nm indicating that the complex contains the ligand. The addition of a droplet of an ammonia solution leads to a decrease in the intensity of the band in a range of 280 nm related, most likely, to the formation of intramolecular hydrogen bonds characteristic of bis(dioximates) favoring the shift of the electron cloud from the aromatic ring to the metallocycle.

In the IR spectrum of Ni(II) bis(dioximate) (**I**), the value ν(OH) 3076 cm^{-1} is a consequence of a strong intramolecular hydrogen bond of the O–H···O type. Since the oxime =NOH groups in the transition metal bis(dioximates) form strong hydrogen bonds of the O–H···O type, the band at 3650–3100 cm^{-1} corresponding to the ν(OH) vibration shifts from a range in the spectra of noncoordinated oxime molecules [30, 32] at 2350 and 2340 cm^{-1}, for example, for $Ni(Dmg)_2$ and $Pd(Dmg)_2$, respectively (Dmg is the dimethylglyoxime anion). The dependence of the ν(OH) frequency on the O–H···O distance was established [30, 32]. The IR spectrum of Cu(II) tris(dioximine) (**II**) contains the following bands (cm^{-1}): 3469–3208 ν(NH), 3071–3075 ν(OH), 1643–1646 ν(C=N), 1588–1595 $\nu(CC)_{arom}$, 900–913 ν(NO), and 741–747 δ(CH). However, both the majority of the above presented bands and the bands characteristic of the ionized oxime group at 1255 and 1093 cm^{-1} are observed in the spectrum of Ni(II) bis(dioximate) (**I**).

The ^1H NMR spectrum of compound **I** contains the signal of the proton of the oxime group confirming the formation of intramolecular hydrogen bonds. The signals of the protons of the NH groups and the carbon atoms of the aromatic rings bound to these groups undergo substantial shifts, which is due to the electron density shift from the dioxime fragments to the metallocycle. The same is observed in the ^{13}C NMR spectra of complexes **I** and **II**.

Compound L crystallizes in the trigonal space group $P3_12_1$ (Table 1). The independent part of the unit cell of L contains 1/2 organic $DsamH_2$ molecule with the C_2 symmetry. The molecular structure of L is shown in Fig. 1. The dioxime fragment of $DsamH_2$ is stabilized in the *anti* (*E,E*) conformation, and the NCCN torsion angles formed by the involvement of the N(1) and N(2) nitrogen atoms are 57.5° and –49.1°, respectively. An analysis of the results in the Cambridge Structural Database [34] indicates similar structures of noncoordinated dioximes crystallized as both neutral molecules and protonated organic cations. The interatomic O–N and N–C distances in the oxime fragments in L unsubstantially differ from similar distances in the neutral and organic cations of the modified dioximes with the amino group [35–38]. For instance, the O–N distance in L is 1.420(3) Å (Table 2), whereas they are 1.434 and 1.422 Å for the neutral *N,N'*-bis(2-(morpholino)ethylamino)glyox-

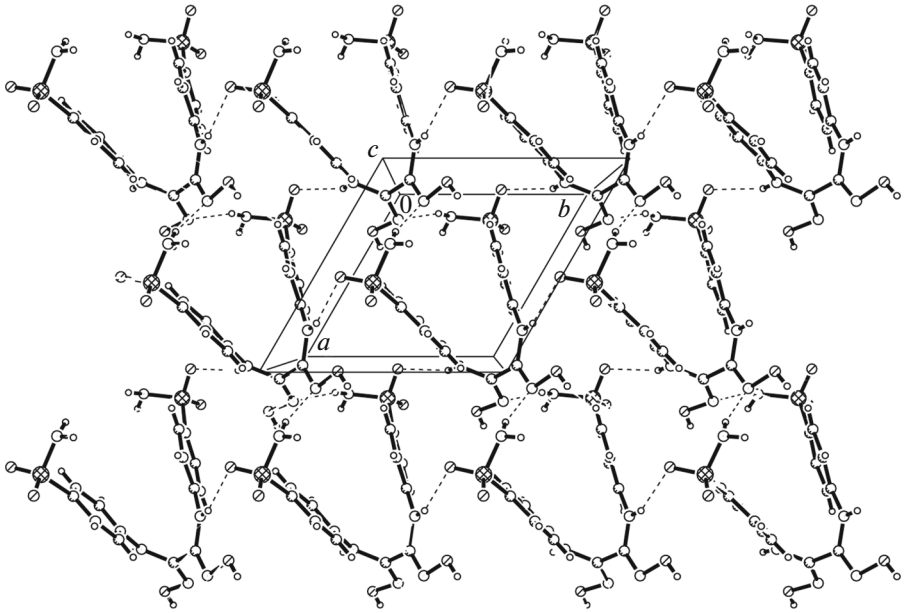

Fig. 2. Joining of the $DsamH_2$ molecules by hydrogen bonds into layers along the *z* axis in the crystal of L.

ime [35] and (2*Z*,3*Z*)-quinoxaline-2,3(1*H*,4*H*)dione-dioxime [36] molecules, respectively.

In the crystal of L, the $DsamH_2$ molecules are joined by a system of O–H···N and N–H···O intermolecular hydrogen bonds (Table 3) involving the OH groups of the oxime fragments and the NH groups of both internal and terminal fragments of the molecule as the proton donors, and the nitrogen atoms of the oxime fragments and the oxygen atoms of the sulfo groups act as the proton acceptors. The formation of different layers can be distinguished in the crystal (Fig. 2).

Compound **II** crystallizes in the monoclinic space group $P2_1/c$. The independent part of the unit cell of compound **II** of the ionic type contains one complex cation $[Cu(DsamH_2)_3]^{2+}$ in the common position (Fig. 3), one SO_4^{2-} anion, and seven crystallization molecules of water, four of which have the filling factor 1/2. The coordination polyhedron of Cu(II) in the complex cation is a distorted tetragonal bipyramid formed by a set of N_6 donor atoms, and all nitrogen atoms belong to the oxime groups of three neutral $DsamH_2$ ligands. Each organic ligand $DsamH_2$ coordinates to the central metal atom via the bidentate-chelating mode to form five-membered metallocycles. The Cu–N bond lengths in the coordination polyhedron range from 1.978(6) to 2.508(5) Å (Table 2). Similar structures were found in the Ni(II) [21, 33, 39–42] and Co(II) [43–46] tris(complexes) in which the derivatives of this ligand are coordinated via the bidentate-chelating mode mainly as the neutral ligand. The $[Cu(DsamH_2)_3]^{2+}$ complex cations are additionally stabilized by weak intramolecular π...π interactions between the aromatic fragments of the ligands, and the centroid...centroid distances in them are 3.580, 3.680, and 3.868 Å.

An analysis of the Cambridge Structural Database [34] revealed the copper monocomplexes and bis(complexes) with oxamidoxime [47–51], one binuclear complex, and one Cu(II) coordination polymer each containing one of these ligands coordinated to each metal atom via the bidentate-chelating mode, and the SO_4^{2-} anions serve as the bridging ligands [49]. Two different monodentate coordination modes were found in the Ni(II) complex with oxamidoxime [52] for the additional sulfanilate ligand: via one O atom and via one N atom. Since the Cambridge Structural Database [34] contains the transition metal complexes with the ligands bearing the benzenesulfamide fragment coordinated via the O or N atom [53, 54], it can be assumed that, under certain conditions, the $DsamH_2$ ligand can be involved in the complex as the bridging ligand.

In the crystal of compound **II**, the $[Cu(DsamH_2)_3]^{2+}$ complex cations, SO_4^{2-} anions, and crystallization molecules of water are joined by a complicated system of intermolecular hydrogen bonds (Table 3) in which the OH groups of the oxime fragments and NH groups involving both the internal and terminal fragments of the complex cations and water molecules as the proton donors, and the nitrogen and oxygen atoms of the terminal SO_2NH_2 groups of the ligands and the O atoms of the SO_4^{2-} anions and crystallization molecules of water act as the proton acceptors. The complex cations are linked to each other by

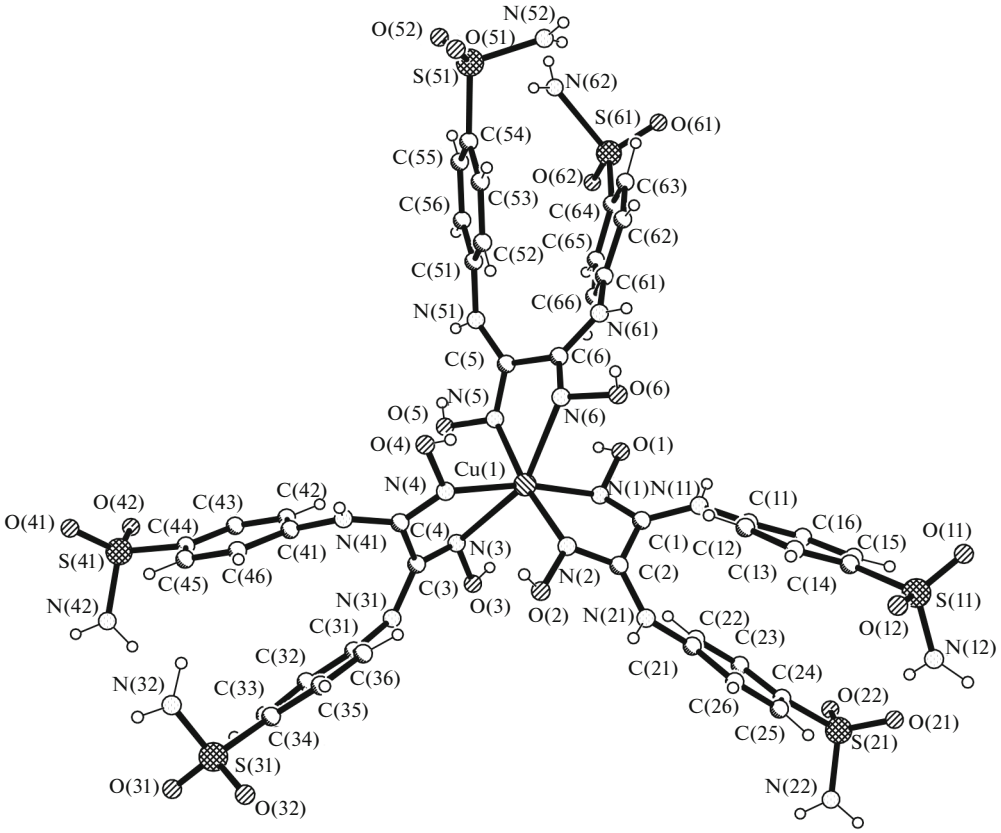

Fig. 3. Structure of the $[Cu(DsamH_2)_3]^{2+}$ complex cation with notation of atoms in compound **II**.

both O–H···O and N–H···O intermolecular hydrogen bonds and weak intermolecular π...π interactions between the aromatic rings of the adjacent molecules (centroid...centroid distance 4.044–4.284 Å). The complex cations are joined by intermolecular hydrogen bonds involving the outer-sphere components: O–H···O with the SO_4^{2-} anion; O–H···O(*w*), N–H···O(*w*), O(*w*)–H···O, and O(*w*)–H···N involving water molecules; and intermolecular hydrogen bonds O(*w*)–H···O between the water molecules and anions (Fig. 4). In the crystal of compound **II**, the $[Cu(DsamH_2)_3]^{2+}$ complex cations and SO_4^{2-} anions are packed rather closely so that the cavities available for crystallization molecules occupy 670.7 Å^3 of the unit cell volume (or 10.2%), whereas the cavities are 989.8 Å^3 of the unit cell volume (or 15.1%) without the comparatively bulky SO_4^{2-} anion. Thus, in compound **II**, the $[Cu(DsamH_2)_3]^{2+}$ complex cations joined by intermolecular hydrogen bonds formed an intrinsic supramolecular structure and the outer SO_4^{2-} anions and crystallization molecules of water are arranged in the cavities by the intermolecular hydrogen bonds stabilizing it and substantially affecting the stability of the whole crystal structure.

The influence of coordination compound **II** on the protease biosynthesis by the strain of the microscopic fungus *Fusarium gibbosum* CNMN FD 12 was studied in dynamics on the 4th, 5th, and 6th days of cultivation: the period corresponding to the biosynthesis maximum of the studied enzymes for the classical producer cultivation.

Upon the addition of the copper complex (**II**) to the nutrient medium, the maximum enzymatic activity is detected at a concentration of 5.0 mg/L on the 5th day of producer cultivation and coincides with the time of appearance of the maximum in the control variant. At this moment, the activity of the acidic proteases is 4.28 units/mL versus 2.77 units/mL in the control, exceeding the control level by 54.5%. As the concentration increases to 10.0 and 15.0 mg/L, the activity of the acidic proteases decreases by 5% on the average compared to the control (Table 4).

The activity of the neutral proteases in the experimental variant significantly exceeds the control level at all tested concentrations being 6.30, 5.96, and 4.79 units/mL, respectively, compared to 3/36 units/mL in the control variant, which is higher than the control level by 42.5–87.5%.

The biosynthesis maximum of the acidic proteases of the mycelium fungus *Trichoderma koningii* Oude-

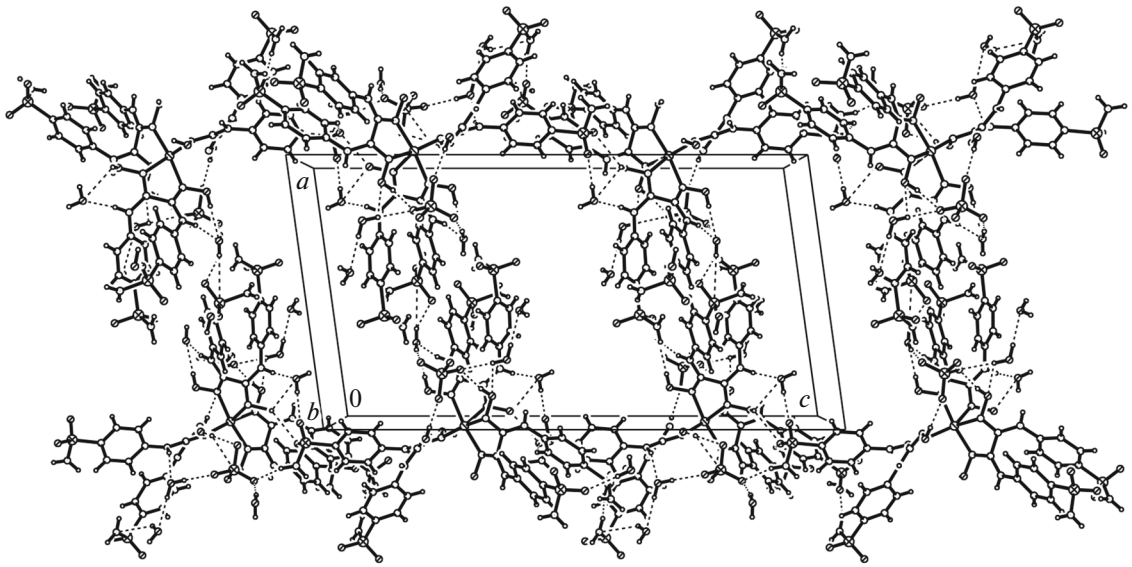

Fig. 4. Fragment of the crystal structure of complex **II**.

mans CNMN FD (1.76–1.93 units/mL) was detected on the 8th day of cultivation exceeding the maximum of the control (1.59 units/mL, 9th day) by 10.7–21.4%. The concentrations favorable for biosynthesis are 5.0 and 10.0 mg/L, and the highest values were achieved at a concentration of 10 mg/L (1.93 units/mL) (Table 5).

The activity maximum of the neutral proteases (4.53 units/mL) at a concentration of the complex of 5.0 mg/L appears on the 9th day of producer cultivation and coincides with the appearance of the biosynthesis maximum in the control variant exceeding the control level by 52.5%. At this concentration, the activity of the neutral proteases is higher than that of the control within the whole cultivation period (8–10th day) exceeding the maximum control level by 36.0% already on the 8th day. For the concentration of the complex equal to 10 mg/L, the activity of the neutral proteases exceeds the control level (by 10.1%) only on the 10th day of cultivation.

Thus, it was revealed that new dioxime (disulfanilamide glyoxime) behaved similarly to dianilineglyoxime: the formation of tris(dioximines) or bis(dioximates) depends on the pH of the solutions. The introduction of additional fragments bearing various functional groups into the dioxime ligand increases its denticity and affects the modes of involving hydrogen bonds in the system. The Cu(II) complex with the $DsamH_2$ ligand taken in optimally selected concentrations provides the stimulating effect on the protease synthesis of the biotechnologically significant micromycete strains *Fusarium gibbosum* CNMN FD 12 and

Table 4. Influence of the Cu(II) complex (**II**) on the proteolytic activity of the micromycete *Fusarium gibbosum* CNMN FD 12

Concentration of coordination compounds (mg/L)	Activity of acidic proteases (pH 3.6)					
	4th day		5th day		6th day	
	units/mL	% of control	units/mL	% of control	units/mL	% of control
5.0	0.25 ± 0.01	50.0	4.28 ± 0.07	154.5	2.02 ± 0.04	171.4
10.0	0.59 ± 0.04	116.7	2.69 ± 0.07	97.0	0.76 ± 0.07	64.3
15.0	0.42 ± 0.01	84.0	2.52 ± 0.07	90.9	0.17 ± 0.01	14.3
Control	0.50 ± 0.04	100.0	2.77 ± 0.04	100.0	1.18 ± 0.07	100.0
	Activity of neutral proteases (pH 7.4)					
5.0	2.02 ± 0.04	160.0	6.30 ± 0.04	187.5	3.53 ± 0.04	140.0
10.0	1.60 ± 0.04	126.7	5.96 ± 0.07	177.5	4.20 ± 0.08	166.7
15.0	1.34 ± 0.07	104.3	4.79 ± 0.04	142.5	2.52 ± 0.07	100.0
Control	1.26 ± 0.01	100.0	3.36 ± 0.07	100.0	2.52 ± 0.04	100.0

Table 5. Influence of the Cu(II) complex (**II**) on the proteolytic activity of the micromycete *Trichoderma koningii* Oudemans CNMN FD 15

Concentration of coordination compounds (mg/L)	Activity of acidic proteases (pH 3.6)					
	8th day		9th day		10th day	
	units/mL	% of control	units/mL	% of control	units/mL	% of control
5.0	1.76 ± 0.03	222.8/110.7*	0.92 ± 0.01	57.9	0.59 ± 0.04	140.5
10.0	1.93 ± 0.01	244.3/121.4*	0.08 ± 0.03	5.0	0.42 ± 0.02	100.0
15.0	0.84 ± 0.04	106.3				
Control	0.79 ± 0.01	100.0	1.59 ± 0.07	100.0	0.42 ± 0.02	100.0
	Activity of neutral proteases (pH 7.4)					
5.0	4.04 ± 0.04	177.9/136.0*	4.53 ± 0.08	152.5	3.15 ± 0.04	138.8
10.0	3.03 ± 0.07	133.5	2.64 ± 0.07	88.9	3.27 ± 0.01	144.1/110.1*
15.0	2.01 ± 0.04	88.5	2.52 ± 0.01	84.8	2.64 ± 0.02	116.3
Control	2.27 ± 0.01	100.0	2.97 ± 0.02	100.0	2.27 ± 0.01	100.0

* Compared to the control of the same day/compared to the maximum value of the control (9th day).

Trichoderma koningii Oudemans CNMN FD 15 increasing the activity of the acidic and neutral proteases by 21.4–54.5 and 52.5–87.5%, respectively, over the control. As a result, this compound is of interest for biotechnological developments as a potential biostimulator of enzyme formation in strains of mycelium fungi producers.

FUNDING

This work was carried out in terms of state assignments (projects nos. 20.80009.5007.15 and 20.80009.5007.28) of the National Agency for Research and Development of Republic of Moldova.

CONFLICT OF INTEREST

The authors declare that they have no conflicts of interest.

REFERENCES

1. Janiak, Ch., *Dalton Trans.*, 2003, p. 2781.
2. Bourosh, P.N., Coropceanu, E.B., Siminov, Yu.A., et al., *Russ. J. Coord. Chem.*, 2002, vol. 28, no. 9, p. 647. https://doi.org/10.1023/A:1020095101054
3. Melnic, E., Coropceanu, E.B., Forni, A., et al., *Cryst. Growth Des.*, 2016, vol. 16, no. 11, p. 6275.
4. Croitor, L., Coropceanu, E.B., Chisca, D., et al., *Cryst. Growth Des.*, 2014, vol. 14, no. 6, p. 3015.
5. Coropceanu, E.B., Croitor, L., and Fonari, M.S., *Polyhedron*, 2012, vol. 38, no. 1, p. 68.
6. Coropceanu, E., Croitor, L., Gdaniec, M., et al., *Inorg. Chim. Acta*, 2009, vol. 362, no. 7, p. 2151.
7. Coropceanu, E.B., Croitor, L., Botoshansky, M.M., et al., *Polyhedron*, 2011, vol. 30, no. 15, p. 2592.
8. Coropceanu, E., Rija, A., Lozan, V., et al., *Cryst. Growth Des.*, 2016, vol. 16, no. 2, p. 814.
9. Croitor, L., Coropceanu, E.B., Siminel, A.V., et al., *CrystEngComm*, 2012, vol. 14, no. 10, p. 3750.
10. Coropceanu, E.B., Croitor, L., Siminel, A.V., et al., *Polyhedron*, 2016, vol. 109, p. 107.
11. Bresciani Pahor, N., Farcolin, M., Marzilli, L.G., et al., *Coord. Chem. Rev.*, 1985, vol. 63, p. 1.
12. Randaccio, L., Bresciani Pahor, N., Zangrando, E., and Marzilli, L.G., *Chem. Soc. Rev.*, 1989, vol. 18, p. 225.
13. Desyatnik, A.A., Gerbeleu, N.V., Koropchanu, E.B., et al., *Russ. J. Coord. Chem*, 2002, vol. 28, no. 2, p. 135. https://doi.org/10.1023/A:1014240303176
14. Bourosh, P.N., Koropchanu, E.B., Ciloci, A.A., et al., *Russ. J. Coord. Chem*, 2009, vol. 35, no. 10, p. 751. https://doi.org/10.1134/S1070328409100078
15. Mokhir, A., Krämer, R., Voloshin, Y.Z., and Varzatskii, O.A., *Bioorg. Med. Chem. Lett.*, 2004, vol. 14, no. 11, p. 2927.
16. Coropceanu, E.B., Bulhac, I.I., Shtefyrtse, A.A., et al., *Russ. J. Coord. Chem.*, 2017, vol. 43, no. 3, p. 164. https://doi.org/10.1134/S1070328417030046
17. Ocak, U., Kantekin, H., Gok, Y., and Misir, M.N., *New J. Chem.*, 2003, vol. 27, p. 1251.
18. Gumus, G., Ahsen, V., Lebrun, C., et al., *New J. Chem.*, 2004, vol. 28, p. 177.
19. Ureche, D., Rija, A., Bulhac, A., et al., *Russ. J. Inorg. Chem.*, 2020, vol. 65, no. 12, p. 1838. https://doi.org/10.1134/S0036023620120189
20. Bourosh, P.N., Coropceanu, E.B., Ciloci, A.A., et al., *Russ. J. Coord. Chem.,* 2013, vol. 39, no. 11, p. 777. https://doi.org/10.1134/S107032841311002X
21. Yuksel, F., Gurek, G., Durmus, M., et al., *Inorg. Chim. Acta*, 2008, vol. 361, no. 8, p. 2225.
22. Rija, A., Bulhac, I., Coropceanu, E., et al., http://www.cjm.asm.md/sites/default/files/article_files/Rija%20016%20.pdf.

23. *CrysAlis RED, O.D.L. Version 1.171.34.76. Data Collection and Processing Software for Agilent X-ray Diffractometers*, 2003.
24. Sheldrick, G.M., *Acta Crystallogr., Sect. A: Found. Crystallogr.*, 2008, vol. 64, no. 1, p. 112.
25. Deseatnic-Ciloci, A., Tiurina, J., Lupascu, G., et al., *Brevet MD 4186*, BOPI 2012, no. 11.
26. Deseatnic-Ciloci, A., Tiurina, J., Lupascu, G., et al., *Brevet MD 4285*, BOPI 2014, no. 5.
27. Gracheva, I.M., Grachev, Yu.P., Mosichev, M.S., et al., *Laboratornyi praktikum po tekhnologii fermentnykh preparatov* (Laboratory Works on the Technology of Enzyme Preparations), Moscow: Legkaya i pishch. Prom., 1982.
28. Dospekhov, B. *Planirovanie polevogo opyta i statich-eskaya obrabotka dannykh* (Planning of Field Experiment and Statistical Data Treatment), Moscow: Kolos, 1985.
29. Bellamy, L.J., *The Infrared Spectra of Complex Molecules*, New York: Wiley, 1958.
30. Gordon, A. and Ford, R., *The Chemist's Companion: A Handbook of Practical Data, Techniques, and References*, New York: Wiley, 1972.
31. Tarasevich, B.N., *IK spektry osnovnykh klassov organicheskikh soedinenii. Spravochnye materialy* (IR Spectra of the Main Classes of Organic Compounds), Moscow, 2012.
32. Nakamoto, K., *Infrared Spectra and Raman Spectra of Inorganic and Coordination Compounds*, New York: Wiley, 1986.
33. Coropceanu, E.B., Ureche, D., Rija, A.P., et al., *Russ. J. Coord. Chem.,* 2021, vol. 47, no. 1, p. 17. https://doi.org/10.1134/S1070328421010024
34. Allen, F.H., *Acta Crystallogr., Sect. B: Struct. Sci.*, 2002, vol. 58, nos. 3–1, p. 380.
35. Durmus, M., Ahsen, V., Luneau, D., and Pecaut, J., *Inorg. Chim. Acta*, 2004, vol. 357, p. 588.
36. Kakanejadifard, A. and Amani, V., *Acta Crystallogr., Sect. E: Struct. Rep. Online*, 2008, vol. 64, p. o1512.
37. Endres, H. and Schendzielorz, M., *Acta Crystallogr., Sect. C: Struct. Struct. Commun.*, 1984, vol. 40, p. 453.
38. Ureche, D., Bulhac, I., Rija, A., et al., *Russ. J. Coord. Chem.,* 2019, vol. 45, no. 12, p. 843. https://doi.org/10.1134/S107032841912008X
39. Belombe, M.M., Nenwa, J., Kammoe, A.L., and Poudeu, P.F.P., *Acta Crystallogr., Sect. E: Struct. Rep. Online*, 2006, vol. 62, p. m2583.
40. Belombe, M.M., Nenwa, J., Mbiangue, Y.A., et al., *Acta Crystallogr., Sect. E: Struct. Rep. Online.*, 2008, vol. 64, p. m1440.
41. Endres, H. and Jannack, T., *Acta Crystallogr., Sect. B: Struct. Crystallogr. Cryst. Chem.*, 1980, vol. 36, p. 2136.
42. Nenwa, J., Djonwouo, P.L., Belombe, M.M., et al., *ScienceJet*, 2013, vol. 2, p. 43.
43. Belombe, M.M., Nenwa, J., Mbiangue, Y.A., et al., *Dalton Trans.*, 2009, p. 4519.
44. Belombe, M.M., Nenwa, J., Bebga, G., et al., *Acta Crystallogr., Sect. E: Struct. Rep. Online.*, 2007, vol. 63, p. m2037.
45. Bekaroglu, O., Sarisaban, S., Koray, A.R., et al., *Acta Crystallogr., Sect. B: Struct. Crystallogr. Cryst. Chem.*, 1978, vol. 34, p. 3591.
46. Belombe, M.M., Nenwa, J., Lonnecke, P., and Hey-Hawkins, E., *Z. Anorg. Allg. Chem.*, 2009, vol. 635, p. 420.
47. Kawata, S., Kitagawa, S., Machida, H., et al., *Inorg. Chim. Acta*, 1995, vol. 229, p. 211.
48. Endres, H., Genc, N., and Nothe, D., *Z. Naturforsch., A: Phys. Sci.*, vol. 38, p. 90.
49. Endres, H., Nothe, D., Rossato, E., and Hatfield, W.E., *Inorg. Chem.*, 1984, vol. 23, p. 3467.
50. Endres, H. and Genc, N., *Acta Crystallogr., Sect. C: Cryst. Struct. Commun.*, 1983, vol. 39, p. 704.
51. Nenwa, J., Djonwouo, P.L., Nfor, E.N., et al., *Z. Naturforsch., B: J. Chem. Sci.*, 2014, vol. 69, p. 321.
52. Endres, H., *Z. Anorg. Allg. Chem.*, 1984, vol. 513, p. 78.
53. Tommasino, J.-B., Pilet, G., Renaud, F.N.R., et al., *Polyhedron*, 2012, vol. 37, p. 27.
54. Xiao, B., Gong, T.-J., Xu, J., et al., *J. Am. Chem. Soc.*, 2011, vol. 133, p. 1466.

Translated by E. Yablonskaya